


# A transmural gradient of myocardial remodeling in early-stage heart failure with preserved ejection fraction in the pig

Christian Mühlfeld,<sup>1,2,3</sup>  Alexandra Rajces,<sup>1</sup> Martin Manninger,<sup>4</sup> Alessio Alogna,<sup>5,6</sup> Marie-Christin Wierich,<sup>1</sup> Daniel Scherr,<sup>4,7</sup> Heiner Post<sup>8</sup> and Julia Schipke<sup>1,2,3</sup>

<sup>1</sup>Institute of Functional and Applied Anatomy, Hannover Medical School, Hannover, Germany

<sup>2</sup>Cluster of Excellence REBIRTH (From Regenerative Biology to Reconstructive Therapy), Hannover, Germany

<sup>3</sup>German Center for Lung Research (DZL), Biomedical Research in Endstage and Obstructive Lung Disease Hannover (BREATH), Hannover, Germany

<sup>4</sup>Division of Cardiology, Department of Medicine, Medical University of Graz, Graz, Austria

<sup>5</sup>Department of Cardiology, Charité University Medicine, Berlin, Germany

<sup>6</sup>Berlin Institute of Health (BIH), Berlin, Germany

<sup>7</sup>Department of Cardiology, Cardiovascular Research Institute Maastricht (CARIM), Maastricht University Medical Center, Maastricht, The Netherlands

<sup>8</sup>Department of Cardiology, Contilia Heart and Vessel Centre, St. Marien-Hospital Mülheim, Mülheim, Germany

## Abstract

Heart failure with preserved ejection fraction (HFpEF) is characterized by diastolic dysfunction. This study aimed to analyze whether early HFpEF is already associated with ultrastructural alterations and whether they differ quantitatively among the layers of the left ventricular wall. HFpEF was induced in pigs by deoxy-corticosterone acetate (DOCA) treatment along with a high-salt/high lipid diet over 3 months and compared with weight-matched normal pigs ( $n = 5$  each). Samples of the left ventricle were taken and processed for light and electron microscopy. Interstitial fibrosis, subcellular composition of cardiomyocytes and mean cardiomyocyte diameter were evaluated by stereology in subendocardial, midmyocardial and subepicardial regions. DOCA enhanced the mean cardiomyocyte diameter in all locations of the ventricle wall to the same degree. The subcellular composition did not differ between the locations and was not altered by DOCA. The volume fraction of interstitium was smaller in the subendocardium of DOCA group than of control group. Within the interstitium, the volume fraction of collagen fibrils (between cardiomyocytes) was increased in the subendocardial and midmyocardial wall layers of the DOCA group but not in the subepicardial layer. Although the capillary length density and average supply area were not altered in response to DOCA in any of the wall layers, the volume fraction of blood vessels related to the interstitial space was enhanced in the subendocardium of the DOCA group but not in the other wall layers. In conclusion, cardiomyocyte changes due to DOCA were similar in subepicardial, midmyocardial and subendocardial regions but DOCA-induced changes in the interstitium appeared to be more pronounced in the subendocardial ventricular wall layers. This suggests a pivotal role of the subendocardial interstitium in the pathogenesis of HFpEF.

**Key words:** electron microscopy; heart failure with preserved ejection fraction; hypertrophy; stereology; ultrastructure.

## Introduction

Heart failure is a pandemic, globally increasing health problem with a high mortality. Risk factors for the development of heart failure are arterial hypertension, diabetes mellitus, obesity, coronary heart disease, tobacco smoking and aging (Dunlay et al. 2009). Heart failure used to be defined by a reduction in left ventricular ejection fraction (heart failure with reduced ejection fraction, HFrEF) until it was recognized that other forms of heart failure with preserved

### Correspondence

Christian Mühlfeld, Institut für Funktionelle und Angewandte Anatomie, Medizinische Hochschule Hannover, Carl-Neuberg-Str. 1, 30625 Hannover, Germany. T: + 49 511 5322878; E: muehlfeld.christian@mh-hannover.de

Accepted for publication 15 October 2019

Article published online 21 November 2019

ejection fraction (HFpEF) exist and have to be distinguished from the classical HFrEF (Ponikowski et al. 2016). HFpEF has come into focus of cardiac research in recent years because of its high prevalence and its non-responsiveness to classical therapeutics which are effective in HFrEF (Tschöpe et al. 2017). The difficulties in treating HFpEF effectively are based on an incomplete understanding of the pathophysiology of this entity. The most unifying observation in HFpEF is diastolic dysfunction with elevated diastolic filling pressures (Reddy & Borlaug, 2016). A current theory relates HFpEF to the existence of various comorbidities including renal failure, metabolic syndrome or COPD, which then cause a systemic endothelial inflammation that leads to muscle wasting, increased pulmonary resistance and diastolic dysfunction of the heart (Tschöpe et al. 2017).

Knowledge about the morphological alterations in HFpEF may provide an insight into the diastolic dysfunction and its pathophysiology. A recent pathological study reported an increase in fibrotic tissue and a reduction of the microvasculature in human autopsy specimens from 124 patients with HFpEF compared with age-matched control patients who had died of non-cardiac causes (Mohammed et al. 2015). However, these alterations have to be regarded as the end-stage of HFpEF and may therefore not be directly related to its development. In humans, the only possible alternative to autopsy material is the use of endomyocardial biopsies, which carries other potential confounders. One study compared endomyocardial biopsies of patients with 'systolic' HF (HFrEF) and 'diastolic' HF (HFpEF) and described an equally high collagen fraction in both conditions but a higher volume fraction of myofibrils in cardiomyocytes of HFpEF hearts (van Heerebeek et al. 2006). These data are interesting as they show that the two types of HF lead to a different pathological phenotype. However, even within the HF groups the authors could find 'subgroups' with low or high collagen volume fractions. These differences may or may not be based on differences in the underlying pathogenesis but may rather be part of the non-randomness of a single biopsy for the whole organ or of the impossibility of relating the biopsy specimen to a comparable location within the wall. Due to the above-mentioned difficulties it is not possible to evaluate whether there is a transmural gradient in the development of pathological changes in human HFpEF. This, however, would be important to better understand the pathogenesis of this disease.

Hence, great efforts have been put into developing animal models of HFpEF. These models not only face the problem that they have to mimic a pathophysiology currently not completely understood but also that the diagnostic criteria of HFpEF in animals are not clearly defined. However, due to the complexity of HFpEF, its chronic character and the anatomy of the heart, large animal models are superior to rodent models in terms of representativeness of the human disease (Conceição et al. 2016). Recently, a pig model of arterial hypertension – based on the implantation

of deoxy-corticosterone acetate (DOCA) pellets in combination with a high-salt, high-sugar and high-fat diet (Schwarzl et al. 2015) or a high-salt and high-sugar diet (Reiter et al. 2016) was introduced which mimics several pathophysiological features of HFpEF, including concentric left ventricular hypertrophy, increased left ventricular end-diastolic pressure, a shift towards the stiffer titin isoform N2B and uncoupled NOS activity (Schwarzl et al. 2015; Reiter et al. 2016).

Since this animal model represents an early disease stage, the present study was carried out on material obtained during the study of Reiter et al. (2016) to characterize the morphological alterations more precisely, and at an early stage of disease development. Specifically, the hypothesis was tested that myocardial remodeling in HFpEF differs between the different layers of the left ventricular wall. Therefore, samples from the subendocardial, midmyocardial and subepicardial regions of the left ventricular free wall were taken and subjected to a quantitative electron microscopic investigation.

## Materials and methods

### Animals

The animal experiments from which the samples of the present study were taken were approved by the local Bioethics Committee of Vienna, Austria (BMWF-66.010/0091-II/3b/2013) and conformed to the guide for the care and use of laboratory animals, US National Institute of Health (NIH Publication No. 85–23, revised 1996). Details of the animal model and experimental procedure were published in Schwarzl et al. (2015) and Reiter et al. (2016). Briefly, 10 female landrace pigs were assigned to a control or DOCA group ( $n = 5$  each). In the latter, arterial hypertension was evoked by subcutaneous implantation of DOCA pellets ( $100 \text{ mg kg}^{-1}$ , 90-day release, Innovative Research of America, USA) in combination with a high-salt, high-sugar, high-potassium diet. The experiments were terminated at 12 weeks after the onset of treatment. After several *in vivo* measurements under appropriate anesthesia (Reiter et al. 2016), a bolus of  $100 \text{ mmol potassium}$  was injected into the coronary arteries to induce cardiac arrest and death of the animals. Subendocardial, midmyocardial and subepicardial samples were taken from the left ventricular free wall (excluding the interventricular septum) and fixed and stored in 1.5% paraformaldehyde, 1.5% glutaraldehyde in  $0.15 \text{ M}$  Hepes buffer at  $4^\circ \text{C}$ .

### Sample processing

The samples were embedded in epoxy resin according to a standard protocol (Mühlfeld et al. 2007) which included postfixation with 1% osmium tetroxide, *en bloc* staining with aqueous half-saturated uranyl acetate, dehydration in an ascending acetone series and finally embedding in epoxy resin. The tissue blocks were dropped randomly into the embedding forms to ensure random orientation (Stringer et al. 1982). From the resin-embedded samples, semithin ( $1 \mu\text{m}$ ) and ultrathin sections ( $60\text{--}80 \text{ nm}$ ) were cut using an ultramicrotome, mounted on glass slides or nickel mesh grids, respectively, and post-stained with toluidine blue for light microscopy (LM) or with uranyl acetate and lead citrate for transmission electron

microscopy (TEM). In each animal, two tissue blocks per location (subendocardial, midmyocardial and subepicardial) were prepared for microscopy.

## Stereology

All stereological parameters were estimated according to the concepts described in Mühlfeld et al. (2010) and Mühlfeld (2014). All investigators were blinded to the experimental groups throughout the analysis. The semithin sections were analyzed using a Leica DM6000B (Leica, Wetzlar, Germany) microscope with an Olympus DP72 digital camera (Olympus, Hamburg, Germany) and a motorized stage operated by the stereology software (Visiopharm, Hørsholm, Denmark). The ultrathin sections were investigated using a Morgagni transmission electron microscope (FEI, Eindhoven, Netherlands) equipped with a digital camera (Veleta, Olympus, Münster, Germany). All fields of view were obtained by systematic uniform random sampling, i.e. starting at a random point all subsequent fields of view are gathered by moving in predefined intervals in the *x* and *y* directions. In contrast to LM, where the stereology software generates the random fields of view automatically, this has to be done manually at the electron microscope. Systematic uniform random sampling ensured that every part of the section had an equal chance of entering the analysis and that no subjective selection of test fields was performed.

The degree of cardiomyocyte hypertrophy was evaluated by estimating the central mean transverse diameter at  $\times 40$  objective lens magnification at the LM. For this purpose, randomly sampled test fields were overlaid with an unbiased counting frame (Gundersen, 1977) and cardiomyocytes were selected for diameter measurement by the presence of a nucleus within the counting frame. To ensure the correct diameter was measured independent of the cutting angle, the largest diameter orthogonal to the longitudinal axis was measured.

At the TEM level, the digital images were overlaid with grids consisting of test points or test planes (unbiased counting frame) for volume or length density estimation, respectively. Specifically, the volume fractions of cardiomyocytes and interstitium (here defined as all cellular and non-cellular structures except cardiomyocytes), cardiomyocyte organelles (mitochondria, myofibrils, sarcoplasm and nuclei), blood vessels and collagen between cardiomyocytes or at other locations (perivascular, perimysial; Fig. 1) were estimated from images taken at  $\times 8900$  primary magnification. The length density of capillaries was estimated from images taken at a primary magnification of  $\times 2800$ . In general, volume densities were calculated by dividing the number of points hitting a structure of interest by the number of points hitting the reference volume. The length density of capillaries was calculated by  $2*Q/A$ , where *Q* is the number of capillary profiles within the unbiased counting frame and *A* is the total counting frame area hitting the reference volume (Mühlfeld et al. 2010).

Stereological data from these samples were included in two previous studies, Reiter et al. (2016) and Schipke et al. (2017). In Reiter et al. (2016), transmural samples were analyzed for correlation with magnetic resonance data. Specifically, the volume fractions of the interstitium, blood vessels and collagen in relation to the left ventricle and the interstitium, as well as the total volume of myocytes, collagen and blood vessels in the left ventricle, were reported. In a methods comparison for the study of cardiac fibrosis, Schipke et al. (2017) reported the volume fractions of collagen both with respect

to the wall layer and the collagen localization in relation to the total myocardial area.

## Statistics

The statistical analysis and the preparation of dot blots were performed using GRAPHPAD PRISM (Version 4.0, Graphpad Software). The data of the control and DOCA groups were compared by the Mann–Whitney *U*-test. Within one group, the data of the different wall layers were compared using one-way analysis of variance (ANOVA) by SIGMA PLOT (version 13.0; Systat Software, Inc.). This comparison was not within the focus of the study, but interested readers may refer to the tables in Supporting Information Tables S1 and S2. Differences were considered statistically significant if  $P < 0.05$ .

## Results

The degree of hypertrophy of cardiomyocytes was similar in all regions of the ventricular wall, as shown by the mean transverse diameter of cardiomyocytes. This parameter was larger in the DOCA group than in the control group in all regions of the wall but it did not show significant differences among wall regions within one group (Fig. 2). In addition, the composition of the cardiomyocytes, as characterized by the volume fractions of myofibrils, mitochondria, sarcoplasm and nuclei, was not different between control and DOCA group in any of the wall locations (Fig. 3). In line with this, the volume fraction of cardiomyocytes and interstitium was similar in the control and DOCA groups both in the subepicardial and midmyocardial region, indicating that the hypertrophic response in the DOCA group applies to both compartments similarly in these regions. However, in the subendocardium the volume fraction of cardiomyocytes was higher and the volume fraction of the interstitium lower in the DOCA group than in the control group. This suggests that the hypertrophic response of cardiomyocytes is larger than the volume increase of the interstitium in the subendocardium, in contrast to the outer wall layers (Fig. 4).

Within the interstitium, differences between control group and DOCA group were not present in the subepicardial layer but were present in the inner regions of the wall. The volume fraction of collagen fibrils located between cardiomyocytes (related to the interstitium as the reference volume) was higher in the DOCA than in the control group but only in the midmyocardial and subendocardial regions (Fig. 5). Similarly, the volume density of blood vessels was significantly higher in DOCA than in control in the subendocardial layer and showed a similar tendency in the midmyocardial layer. The length density of capillaries did not differ in any of the wall layers between control and DOCA group. Consequently, the reciprocal of the length density, a measure of the mean supply area of an individual capillary, was not different between the groups in any of the layers (Fig. 6).

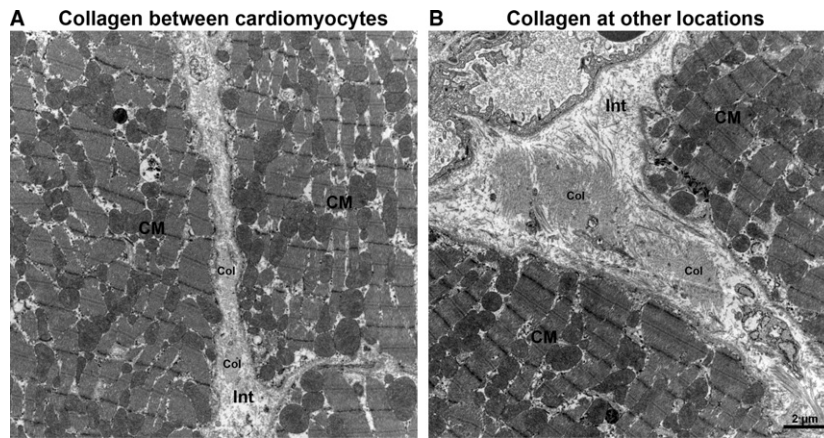


**Fig. 1** Differentiation of collagen localization. Collagen was quantified at different locations, namely, between cardiomyocytes (A) and at other locations including perimysial and perivascular collagen (B). CM, cardiomyocytes; col, collagen fibrils; Int, interstitium.

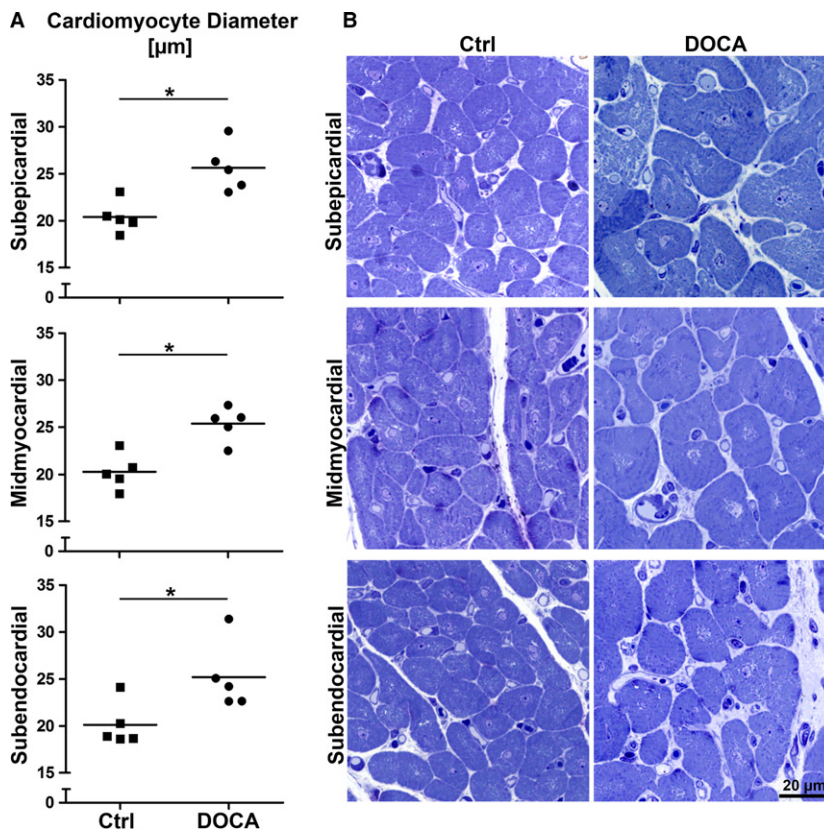


**Fig. 2** Mean cardiomyocyte transverse diameter. (A) Mean transverse cardiomyocyte diameter for control and DOCA group in subepicardial, midmyocardial and subendocardial left ventricle wall. (B) Representative light micrographs of transversally sectioned cardiomyocytes corresponding to the data shown in (A). \*Significant difference between control and DOCA ( $P < 0.05$ ). Each symbol represents the data of a single animal; horizontal bars represent group means.

Overall, the results showed that cardiomyocyte hypertrophy in the DOCA group occurred in all regions of the wall to a similar degree; however, within the interstitium, differences between control and DOCA animals suggested a transmural gradient with changes mainly in the subendocardium and less pronounced in the midmyocardial layer.

## Discussion

The present study provides a comprehensive analysis of transmural quantitative differences of remodeling in the left ventricle of a large animal model of HFpEF. The concentric remodeling of the left ventricle was characterized by an

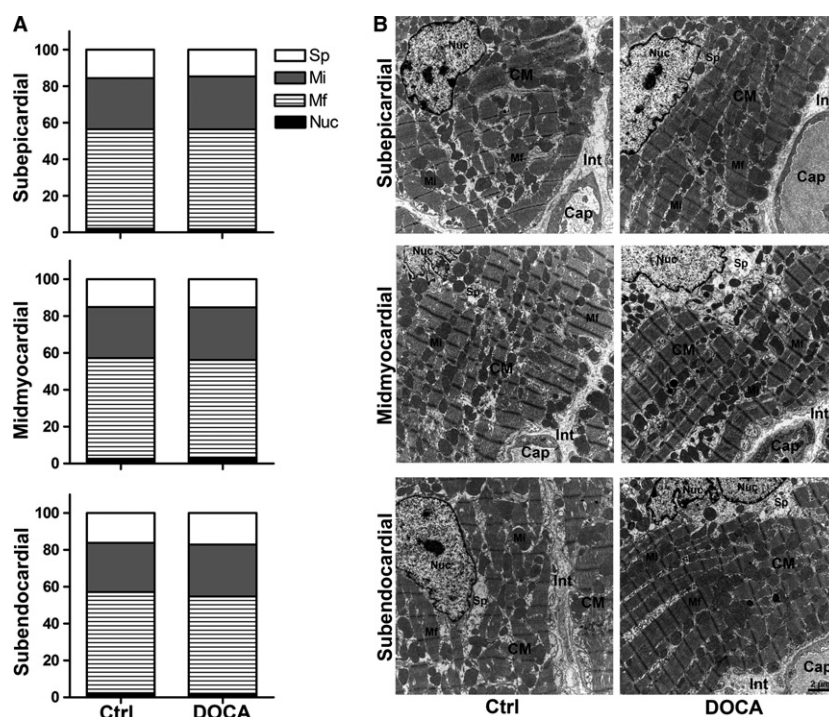


**Fig. 3** Relative composition of subcellular cardiomyocyte compartments. (A) Volume fractions of myofibrils (Mf), mitochondria (Mi), nuclei (Nuc) and free sarcoplasm (Sp) for control and DOCA group in subepicardial, midmyocardial and subendocardial left ventricle wall. Volume fractions were related to the cardiomyocyte as the reference volume. (B) Representative electron micrographs of cardiomyocyte ultrastructure corresponding to the data shown in (A). Each symbol represents the data of a single animal; horizontal bars represent group means. Cap, capillary; CM, cardiomyocytes; Int, interstitium.

increased transverse cardiomyocyte diameter but a similar subcellular composition in all three layers of the wall. However, differences among the layers were observed in the non-cardiomyocyte compartments, with only subtle alterations in the subepicardial and midmyocardial but significant changes in the subendocardial regions of the left ventricular wall. The volume fractions of collagen fibrils and blood vessels were markedly higher in the subendocardial region of DOCA pigs than control pigs. These data suggest that the cardiomyocyte and non-cardiomyocyte compartments respond differently: although the cardiomyocyte hypertrophic remodeling was similar in all regions, the blood vessels and the interstitium showed more pronounced changes in the inner regions of the ventricular wall.

The present study used a morphometric approach using stereology, which is considered the gold standard of quantitative morphology (Hsia et al. 2010; Mühlfeld et al. 2010). Although the microscopy evaluation was performed according to well established standards of stereology, interpretation of the data has to be done with caution. First of all, samples were not taken randomly from the whole ventricle but only from approximately the same region of the left ventricular free wall. This means that at other locations nearer to the base or the apex of the heart, remodeling may be more or less pronounced (Mayhew, 2008). Secondly,

due to the analysis of different layers of the ventricular wall there was no possibility to measure the volume of the reference space to which the data could be related; therefore, the presented volume fractions are only relative values and every interpretation of these as total values is prone to the reference trap (Hyde et al. 2007). For example, an increase in the volume fraction of, say, collagen fibrils, can be caused by an increase in the amount of collagen fibrils but also by a decrease in the volume of other components of the reference space. In the present study, the volume fraction of the interstitium was lower in the subendocardium of the DOCA group than the control group. In contrast, the volume fraction of collagen fibrils within the interstitium was greater in DOCA than in control subendocardium. In combination this suggests that the hypertrophic increase in the subendocardial collagen fibrils is stronger than in other interstitial compartments.

The animal model used in the current paper is based on a combination of pharmacological and alimentary induced arterial hypertension and hyperlipidemia (Schwarzl et al. 2015). The hypertension was induced by the aldosterone analog DOCA. HFpEF is regarded as a multifactorial disease related to arterial hypertension, diabetes mellitus, obesity, coronary heart disease, tobacco smoking and aging (Dunlay et al. 2009). Although the present model mimics some of the functional characteristics of HFpEF (Schwarzl et al. 2015;

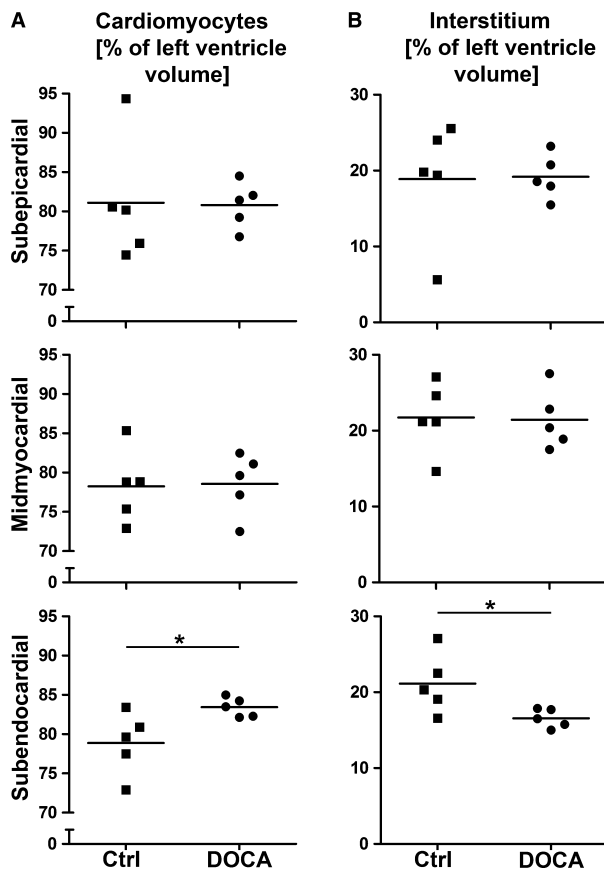


**Fig. 4** Cardiomyocyte and interstitial volume fraction. Volume fractions for control and DOCA group in subepicardial, midmyocardial and subendocardial left ventricle wall. Volume fractions were related to the left ventricular wall as the reference volume. (A) Volume fraction of cardiomyocytes. (B) Volume fraction of interstitium. \*Significant difference between control and DOCA group ( $P < 0.05$ ). Each symbol represents the data of a single animal; horizontal bars represent group means.

Reiter et al. 2016), it cannot be excluded that some of the morphological data reported in the current manuscript are due to a direct pharmacological effect of the DOCA or a reaction to only one of the physiological changes.

In a recent study in the same animal model, we reported quantitative data of the myocardial composition in relation to the whole left ventricle (Reiter et al. 2016), i.e. the data could be multiplied by the volume of the left ventricle as the reference volume; both cardiomyocyte and collagen fibril total volumes were significantly enhanced in the DOCA group. A comparison with the relation between cardiomyocyte and interstitial volume densities reported in the present study shows that the hypertrophic response in the midmyocardial and subepicardial regions was similar for both cardiomyocytes and interstitium. In the subendocardial region, however, the ratio between the two compartments was shifted significantly towards the cardiomyocytes, suggesting that in the subendocardial region the hypertrophic response of cardiomyocytes exceeded that of the

interstitium. Interestingly, however, the relative composition of the cardiomyocytes was not different between DOCA and control group in any location, which suggests that it was not the cardiomyocyte remodeling that differed between inner and outer layers of the wall.

In contrast to the volume fractions of collagen reported here, data on the same animals we reported previously rather showed a tendency towards higher volume fractions in the subepicardial and midmyocardial layers (Schipke et al. 2017). At first glance, this seems to be a contradiction. However, the data in Schipke et al. (2017) were related to the whole left ventricle as the reference volume (including interstitium and cardiomyocytes), whereas the present study related the collagen volume to the volume of the interstitium. As explained above, the subendocardial interstitial volume fraction was significantly lower in the DOCA group but not in the other layers. As a consequence, our collagen data reported in Schipke et al. (2017) are not as conclusive as the current ones, as they do not differentiate between cardiomyocyte and interstitial volume shifts. Although it is not possible to conclude a fibrotic response in the subendocardium based on these data, the DOCA-induced changes of the interstitium are more pronounced in the subendocardial ventricular wall layers, thus suggesting an important role in the pathogenesis of HFpEF.

In dogs with heart failure induced by pressure overload, it was shown that multifocal fibrosis occurred preferentially in the subendocardial region, which was attributed to a subendocardial exhaustion of blood flow reserve and consecutive ischemia (Hittinger et al. 1989). This model of heart failure was based on aortic banding with or without arteriovenous shunt and represented a form of HFpEF. Similarly, in HFpEF patients with aortic valve stenosis, myocardial enlargement with reduction of myofibrils was accompanied by fibrotic tissue (Schaper & Schaper, 1983). In contrast, in the model of HFpEF of the present study, there were no signs of ischemic injury, loss of myofibrils or foci of fibrosis as a result of ischemic cardiomyocyte cell death, which distinguishes the fibrosis observed by Hittinger et al. (1989) and Schaper & Schaper (1983) from the diffuse and mild increase in collagen fibrils observed here. On the other hand, the study by Mohammed et al. (2015) described rarefaction of coronary microvessels in HFpEF patients, indicating that ischemia may also be involved in HFpEF. The autopsy material studied by Mohammed and co-workers presents the end-stage of HFpEF and therefore can not directly be related to the data of the present study from an animal model with an early stage of left ventricular hypertrophy. The present study did not provide evidence for a rarefaction of the supplying capillaries in early HFpEF. This difference may be a direct consequence of the disease stage; for example, it could be that the increase in subendocardial blood vessel volume density is only an early phenomenon attempting to improve perfusion, which may be lost at later stages. Similarly, there was no significant

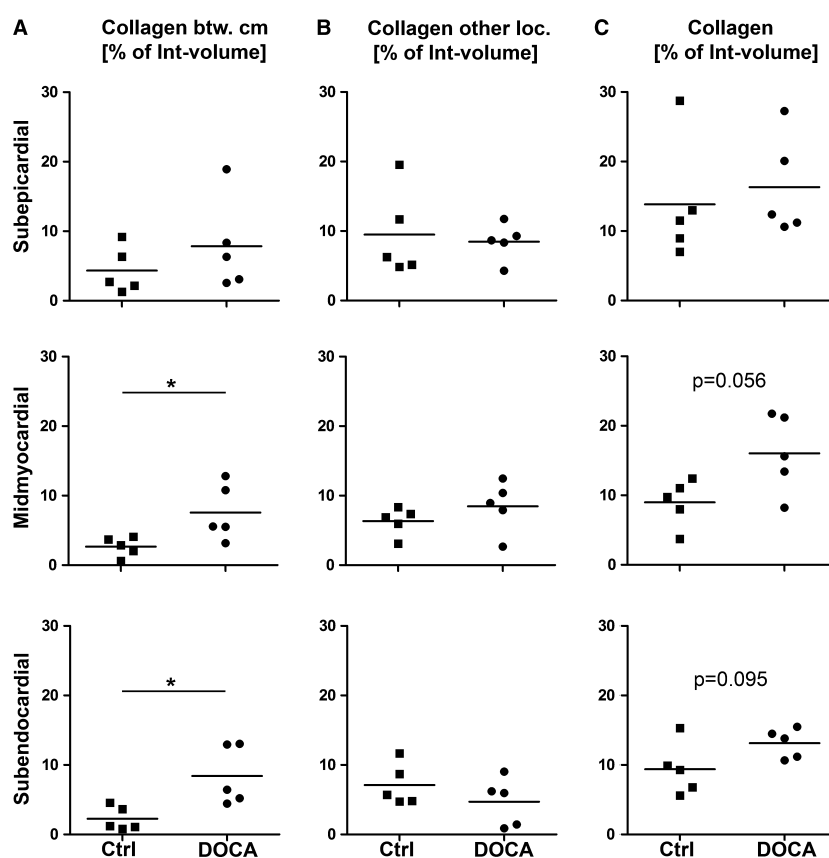


**Fig. 5** Collagen fibril volume fraction. Volume fractions for control and DOCA group in subepicardial, midmyocardial and subendocardial left ventricle wall. Volume fractions were related to the interstitium as the reference volume. (A) Volume fraction of collagen fibrils between cardiomyocytes. (B) Volume fraction of collagen fibrils at other locations (perimysial, perivascular). (C) Volume fraction of all collagen fibrils in the left ventricle. \*Significant difference between control and DOCA group ( $P < 0.05$ ). If  $0.05 < P < 0.1$ , the  $P$ -value was also given to indicate a statistical tendency to a group difference. Each symbol represents the data of a single animal; horizontal bars represent group means.

difference in the capillary length density between the layers of the wall, which is in accordance with a transmural investigation of the microvasculature in normal dogs (Hyde & Buss, 1986). However, a recent study in newly diagnosed untreated hypertensive patients indicated that this disease is associated with a reduced coronary flow reserve (Ikonomidis et al. 2015; Tschöpe & Post, 2015).

Besides the location of fibrous tissue within the ventricular wall, its localization in relation to cardiomyocytes has to be taken into account (Swan, 1994). Although cardiomyocyte death leads to replacement fibrosis, there seems to be a more subtle deposition of collagen at sites with previously less pronounced occurrence of collagen fibers, such as the space between cardiomyocytes (Weber & Brilla 1991). The latter has been observed in a rat model of renovascular hypertension where diastolic dysfunction preceded the loss of systolic capacity and the reduction of ejection fraction (Capasso et al. 1990). As described previously (Schipke et al. 2017), the electron microscopic approach enabled us to discriminate between collagen in the small spaces between cardiomyocytes and larger areas, such as the perivascular or perimysial spaces. Thus, it could be shown that the main

increase in collagen content occurs between cardiomyocytes and is probably linked to the diastolic dysfunction of the left ventricle in HFpEF. As the changes in the interstitial compartment seem to be more pronounced in the subendocardial layer, it is likely that the subendocardium contributes more to the HFpEF phenotype than the outer layers, but it does not seem to be the driver of the overall response. Similar results were recently reported in a pig model with three different comorbidities, namely hypertension, hypercholesterolemia and diabetes mellitus (Sorop et al. 2018). Because of the role of angiotensin in hypertensive cardiac remodeling and fibrosis, which is illustrated by the anti-remodeling effects of angiotensin converting enzyme (ACE) or receptor inhibitors (Ferrario, 2016), it may be speculated that the subendocardial layers may be more susceptible as they are exposed to angiotensin both from the ventricular lumen and the myocardial capillaries. However, the role of an inhibition of the renin-aldosterone-angiotensin system in patients with HFpEF is currently still unclear (Khan et al. 2017; Martin et al. 2018).

In conclusion, DOCA induced changes of cardiomyocytes (diameter, subcellular composition) in all layers of

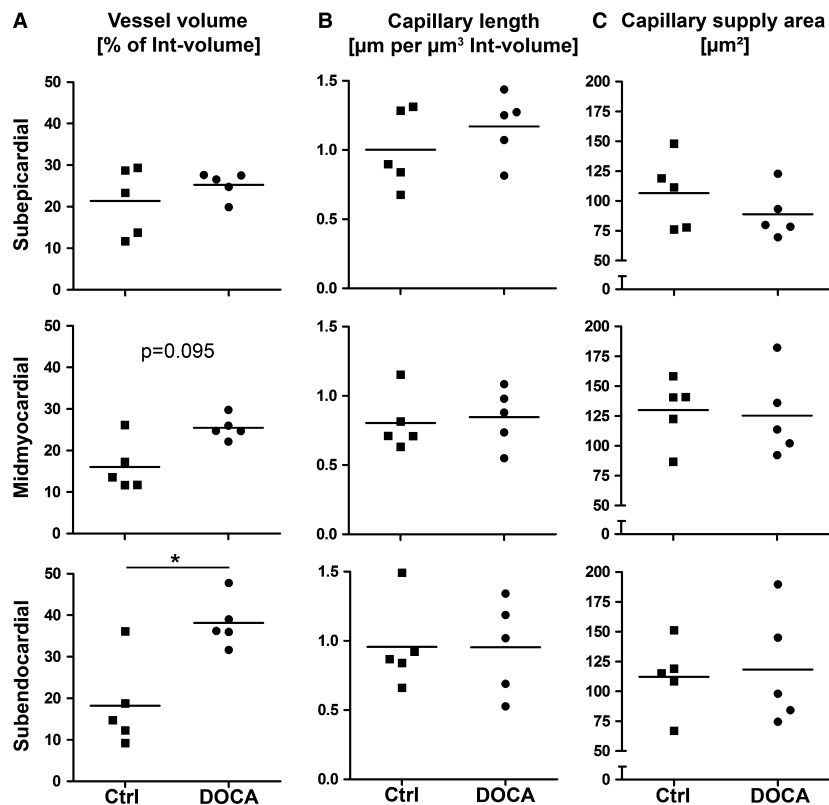


**Fig. 6** Volume fraction of blood vessels and length density of capillaries. Volume fractions, length densities and mean capillary supply area for control and DOCA group in subepicardial, midmyocardial and subendocardial left ventricle wall. Densities were related to the interstitium as the reference volume. (A) Volume fraction of blood vessels, including arterioles, capillaries and venules. (B) Length density of capillaries. (C) Mean capillary supply area. \*Significant difference between control and DOCA group ( $P < 0.05$ ). If  $0.05 < P < 0.1$ , the  $P$ -value was also given to indicate a statistical tendency to a group difference. Each symbol represents the data of a single animal; horizontal bars represent group means.

the left ventricular free wall. The degree of these changes did not differ between the layers of the ventricular wall. In contrast, the interstitium of the subendocardium differed from the outer wall layers regarding volume fraction of interstitium and intermyocytic collagen, and blood vessels (related to interstitium). Only minor alterations were present in the midmyocardial interstitium. These data suggest that early changes in HFpEF are related to the interstitium of the subendocardium of the left ventricle.

## Acknowledgements

The authors gratefully acknowledge the expert technical assistance of Rita Lichatz and Christa Lichtenberg (Hannover). The results of the current work are part of the medical thesis of Alexandra Rajces. This work was supported by the European Union [grant no. 261057, European Network for Translational Research in Atrial Fibrillation (EUTRAF)] and the Deutsche Forschungsgemeinschaft (DFG) via the Cluster of Excellence REBIRTH (EXC62).

## Conflict of interest

The authors declare that there are no conflicts of interest.

## Author contributions

C.M. and J.S. contributed to conception and design of the study, acquisition, interpretation and analysis of data, and to drafting the manuscript. A.R. and M.C.W. contributed to acquisition and analysis of data and to revising the manuscript critically of important intellectual content. M.M., A.A., D.S. and H.P. contributed to conception and design of the study, acquisition, interpretation and analysis of data and to revising the manuscript critically for important intellectual content. All authors have read the manuscript and given final approval to the submitted version.

## References

- Capasso JM, Palakal T, Olivetti G, et al. (1990) Left ventricular failure induced by long-term hypertension in rats. *Circ Res* **60**, 1400–1412.
- Conceição G, Heinonen I, Lourenço AP, et al. (2016) Animal models of heart failure with preserved ejection fraction. *Neth Heart J* **24**, 275–286.
- Dunlay SM, Weston SA, Jacobsen SJ, et al. (2009) Risk factors for heart failure: a population-based case-control study. *Am J Med* **122**, 1023–1028.



- Ferrario CM** (2016) Cardiac remodelling and RAS inhibition. *Ther Adv Cardiovasc Dis* **10**, 162–171.
- Gundersen HJG** (1977) Notes on the estimation of the numerical density of arbitrary profiles: the edge effect. *J Microsc* **111**, 219–223.
- Heerebeek L van, Borbély A, Niessen HW, et al.** (2006) Myocardial structure and function differ in systolic and diastolic heart failure. *Circulation* **113**, 1966–1973.
- Hittinger L, Shannon RP, Bishop SP, et al.** (1989) Subendomyocardial exhaustion of blood flow reserve and increased fibrosis in conscious dogs with heart failure. *Circ Res* **65**, 971–980.
- Hsia CC, Hyde DM, Ochs M, et al.** (2010) An official research policy statement of the American Thoracic Society/European Respiratory Society: standards for quantitative assessment of lung structure. *Am J Respir Crit Care Med* **181**, 394–418.
- Hyde DM, Buss DD** (1986) Morphometry of the coronary microvasculature of the canine left ventricle. *Am J Anat* **177**, 415–425.
- Hyde DM, Tyler NK, Plopper CG** (2007) Morphometry of the respiratory tract: avoiding the sampling, size, orientation, and reference traps. *Toxicol Pathol* **35**, 41–48.
- Ikonomidis I, Tzortzis S, Triantafyllidi H, et al.** (2015) Association of impaired left ventricular twisting-untwisting with vascular dysfunction, neurohumoral activation and impaired exercise capacity in hypertensive heart disease. *Eur J Heart Fail* **17**, 1240–1251.
- Khan MS, Fonarow GC, Khan H, et al.** (2017) Renin-angiotensin blockade in heart failure with preserved ejection fraction: a systematic review and meta-analysis. *ESC Heart Fail* **4**, 402–408.
- Martin N, Manoharan K, Thomas J, et al.** (2018) Beta-blockers and inhibitors of the renin-angiotensin aldosterone system for chronic heart failure with preserved ejection fraction. *Cochrane Database Syst Rev* (6), CD012721.
- Mayhew TM** (2008) Taking tissue samples from the placenta: an illustration of principles and strategies. *Placenta* **29**, 1–14.
- Mohammed SF, Hussain S, Mirzoyev SA, Edwards WD, Maleszewski JJ, Redfield MM** (2015) Coronary microvascular rarefaction and myocardial fibrosis in heart failure with preserved ejection fraction. *Circulation* **131**, 550–559.
- Mühlfeld C** (2014) Quantitative morphology of the vascularisation of organs: a stereological approach illustrated using the cardiac circulation. *Ann Anat* **196**, 12–19.
- Mühlfeld C, Rothen-Rutishauser B, Vanhecke D, et al.** (2007) Visualization and quantitative analysis of nanoparticles in the respiratory tract by transmission electron microscopy. *Part Fibre Toxicol* **4**, 11.
- Mühlfeld C, Nyengaard JR, Mayhew TM** (2010) A review of state-of-the-art stereology for better quantitative 3D morphology in cardiac research. *Cardiovasc Pathol* **19**, 65–82.
- Ponikowski P, Voors AA, Anker SD, et al.** (2016) ESC Guidelines for the diagnosis and treatment of acute and chronic heart failure: the task force for the diagnosis and treatment of acute and chronic heart failure of the European Society of Cardiology (ESC) Developed with the special contribution of the Heart Failure Association (HFA) of the ESC. *Eur Heart J* **37**, 2129–2200.
- Reddy YN, Borlaug BA** (2016) Heart failure with preserved ejection fraction. *Curr Probl Cardiol* **41**, 145–188.
- Reiter U, Reiter G, Manninger M, et al.** (2016) Early-stage heart failure with preserved ejection fraction in the pig: a cardiovascular magnetic resonance study. *J Cardiovasc Magn Reson* **18**, 63.
- Schaper J, Schaper W** (1983) Ultrastructural correlates of reduced cardiac function in human heart disease. *Eur Heart J* **4**(Suppl A), 35–42.
- Schipke J, Brandenberger C, Rajces A, et al.** (2017) Assessment of cardiac fibrosis: a morphometric method comparison for collagen quantification. *J Appl Physiol* (1985) **122**, 1019–1030.
- Schwarzl M, Hamdani N, Seiler S, et al.** (2015) A porcine model of hypertensive cardiomyopathy: implications for heart failure with preserved ejection fraction. *Am J Physiol Heart Circ Physiol* **309**, H1407–H1418.
- Sorop O, Heinonen I, van Kranenburg M, et al.** (2018) Multiple common comorbidities produce left ventricular diastolic dysfunction associated with coronary microvascular dysfunction, oxidative stress, and myocardial stiffening. *Cardiovasc Res* **114**, 954–964.
- Stringer BMJ, Wynford-Thomas D, Williams ED** (1982) Physical randomisation of tissue architecture: an alternative to systematic sampling. *J Microsc* **126**, 179–182.
- Swan HJ** (1994) Left ventricular dysfunction in ischemic heart disease: fundamental importance of the fibrous matrix. *Cardiovasc Drugs Ther* **8**, 305–312.
- Tschöpe C, Post H** (2015) Latent ischaemia as a trigger for a circulus vitiosus of inflammation, fibrosis, and stiffness in HFPEF. *Eur J Heart Fail* **17**, 1210–1212.
- Tschöpe C, van Linthout S, Kherad B** (2017) Heart failure with preserved ejection fraction and future pharmacological strategies: a glance in the crystal ball. *Curr Cardiol Rep* **19**, 70.
- Weber KT, Brilla CG** (1991) Pathological hypertrophy and cardiac interstitium. Fibrosis and renin-angiotensin-aldosterone system. *Circulation* **83**, 1849–1865.

## Supporting Information

Additional Supporting Information may be found in the online version of this article:

**Table S1.** Stereological data of the control group.

**Table S2.** Stereological data of the DOCA group.